



**HAL**  
open science

## **PFKFB4 controls embryonic patterning via Akt signalling independently of glycolysis.**

Caterina Pegoraro, Ana Leonor Figueiredo, Frédérique Maczkowiak, Celio Pouponnot, Alain Eychène, Anne Monsoro-Burq

► **To cite this version:**

Caterina Pegoraro, Ana Leonor Figueiredo, Frédérique Maczkowiak, Celio Pouponnot, Alain Eychène, et al.. PFKFB4 controls embryonic patterning via Akt signalling independently of glycolysis.. Nature Communications, 2014, 6, pp.5953. 10.1038/ncomms6953 . hal-01183654

**HAL Id: hal-01183654**

**<https://hal.science/hal-01183654v1>**

Submitted on 30 Oct 2024

**HAL** is a multi-disciplinary open access archive for the deposit and dissemination of scientific research documents, whether they are published or not. The documents may come from teaching and research institutions in France or abroad, or from public or private research centers.

L'archive ouverte pluridisciplinaire **HAL**, est destinée au dépôt et à la diffusion de documents scientifiques de niveau recherche, publiés ou non, émanant des établissements d'enseignement et de recherche français ou étrangers, des laboratoires publics ou privés.

ARTICLE

Received 30 May 2014 | Accepted 26 Nov 2014 | Published 20 Jan 2015

DOI: 10.1038/ncomms6953

# PFKFB4 controls embryonic patterning via Akt signalling independently of glycolysis

Caterina Pegoraro<sup>1,2,3,4,\*</sup>, Ana Leonor Figueiredo<sup>1,2,3,4,\*</sup>, Frédérique Maczkowiak<sup>1,2,3,4</sup>, Celio Pouponnot<sup>1,2,3,4</sup>, Alain Eychène<sup>1,2,3,4</sup> & Anne H. Monsoro-Burq<sup>1,2,3,4</sup>

How metabolism regulators play roles during early development remains elusive. Here we show that PFKFB4 (6-phosphofructo-2-kinase/fructose-2,6-bisphosphatase 4), a glycolysis regulator, is critical for controlling dorsal ectoderm global patterning in gastrulating frog embryos via a non-glycolytic function. PFKFB4 is required for dorsal ectoderm progenitors to proceed towards more specified fates including neural and non-neural ectoderm, neural crest or placodes. This function is mediated by Akt signalling, a major pathway that integrates cell homeostasis and survival parameters. Restoring Akt signalling rescues the loss of PFKFB4 *in vivo*. In contrast, glycolysis is not essential for frog development at this stage. Our study reveals the existence of a PFKFB4-Akt checkpoint that links cell homeostasis to the ability of progenitor cells to undergo differentiation, and uncovers glycolysis-independent functions of PFKFB4.

<sup>1</sup>Université Paris Sud, Batiment 110, F-91 405 Orsay cedex, France. <sup>2</sup>Institut Curie, Centre Universitaire, Batiment 110, F-91 405 Orsay cedex, France. <sup>3</sup>CNRS UMR3347, Centre Universitaire, Batiment 110, F-91 405 Orsay cedex, France. <sup>4</sup>INSERM U1021, Centre Universitaire, Batiment 110, F-91 405 Orsay cedex, France. \*These authors contributed equally to this work. Correspondence and requests for materials should be addressed to A.H.M.-B. (email: anne-helene.monsoro-burq@curie.fr).

Embryonic patterning involves the complex interplay of multiple signalling pathways triggering gene regulatory networks, which, in turn, drive cell-fate choices and progenitor cell differentiation. While cancer cell metabolism is linked to cancer progression<sup>1–6</sup>, it remains unknown whether the homeostatic balance of progenitor cells affects their ability to undergo differentiation programmes. In particular, the cell metabolic status, its proliferative state and the activity of survival pathways could be important checkpoints for cell patterning progression during development. PFKFB1–4, a highly conserved family of bifunctional kinases/phosphatases, optimizes the cellular rate of glycolysis<sup>7,8</sup>. We found that *pfkfb4* expression is enriched at the dorsal side of frog and chick embryos during early development<sup>9</sup>. However, glucose is not the main source of energy in embryos: the early frog embryo uses yolk-derived amino acids to fuel directly the citric acid cycle in the mitochondria<sup>10,11</sup>. This raised the intriguing possibility that PFKFB4 could play novel roles in dorsal ectoderm formation, besides its classical function on glycolysis regulation.

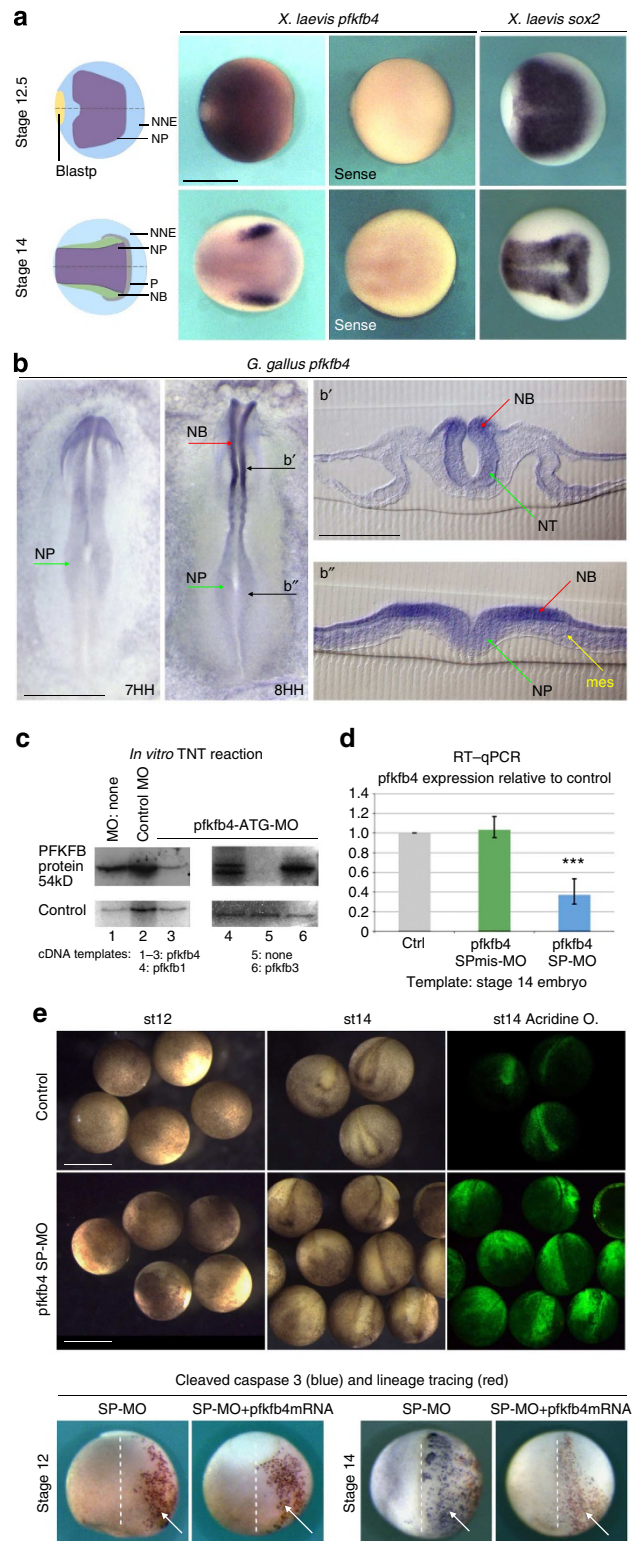
Here, we demonstrate that PFKFB4 levels control the switch of immature ectoderm progenitors towards specified dorsal fates, including neural plate, neural crest, placodes and non-neural ectoderm, in a glycolysis-independent manner. In contrast, we find that PFKFB4 regulates Akt phosphorylation *in vivo*, that the drug-mediated inhibition of Akt phenocopies the PFKFB4 morphant phenotype and that Akt activation rescues the patterning defects in morphant embryos. As PFKFB4-dependent Akt signalling is essential for the progression of embryonic patterning, we propose that PFKFB4 is a pivotal and multi-functional regulator linking cell homeostasis and survival to progenitor cell patterning.

### Figure 1 | *Pfkfb4* is enriched in the developing dorsal ectoderm and is required for its survival during neurulation.

(a) Dorsal ectoderm territories are schematized in *X. laevis* late gastrulas (stage 12.5) and mid-neurulas (stage 14): non-neural ectoderm (NNE), neural plate (NP), neural border (NB), preplacodal ectoderm (P) and blastopore (Blastp). In late gastrulas, *pfkfb4* is expressed broadly dorsally, encompassing *sox2* pan-neural expression. Later, *pfkfb4* is weak in the NP and enriched at the NB, *sox2* marks the NP. WISHs are shown with antisense and control sense probes. Scale bar, 1 mm. Additional views are shown in Supplementary Fig. 2. (b) *pfkfb4* is similarly enriched in the NP of *G. gallus* late gastrulas (stage 6–7HH) and NB of early neurulas (stage 8HH). In contrast, mesoderm (mes) is barely stained as seen on stage 8HH chick transverse sections (b', b''). Scale bars, (b) 1 mm (b', b''): 0.3 mm. (c) Translation-blocking *pfkfb4* ATG-MO specifically decreases PFKFB4 protein synthesis using *in vitro* transcription and translation (TNT) assay, from cDNA template. (d) Splice-blocking *pfkfb4* MO depletes endogenous *pfkfb4* mRNA *in vivo* (RT-qPCR). *P* values were generated using ANOVA test ( $P < 0.001$ ) and error bars represent s.e.m. Controls include control MO (c and d), *pfkfb1* or *pfkfb3* cDNA templates (c). At least three independent experiments were performed. (e) PFKFB4 morphant phenotype: morphology and cell death analysis by acridine orange staining (green staining) and activated caspase-3 immunostaining (blue staining), (14 independent experiments, a total of 649 embryos were analysed and detailed statistical analysis is available in Supplementary Table 2). While morphant embryos undergo marked cell death in the injected area after stage 13–14, restoring *pfkfb4* mRNA rescues the death phenotype (8% of embryos show dead cells before stage 13; 90% of morphant embryos with increased cell death at stage 14 (10% normal embryos); only 45% of embryos with dead cells at stage 14 after *pfkfb4* mRNA coinjection (55% normal embryos as depicted). Arrows mark the injected cells, traced using beta-galactosidase staining (in red, see Methods).

## Results

**PFKFB4 is essential for dorsal ectoderm development.** During vertebrate gastrulation and neurulation, the dorsal ectoderm is patterned into several cell fates: neural plate (NP), non-neural ectoderm (NNE), neural crest (NC) and preplacodal ectoderm (P), a prerequisite for the differentiation of the central and peripheral nervous systems and surrounding tissues. Focusing on genes enriched dorsally during neurulation<sup>9,12</sup>, we found that



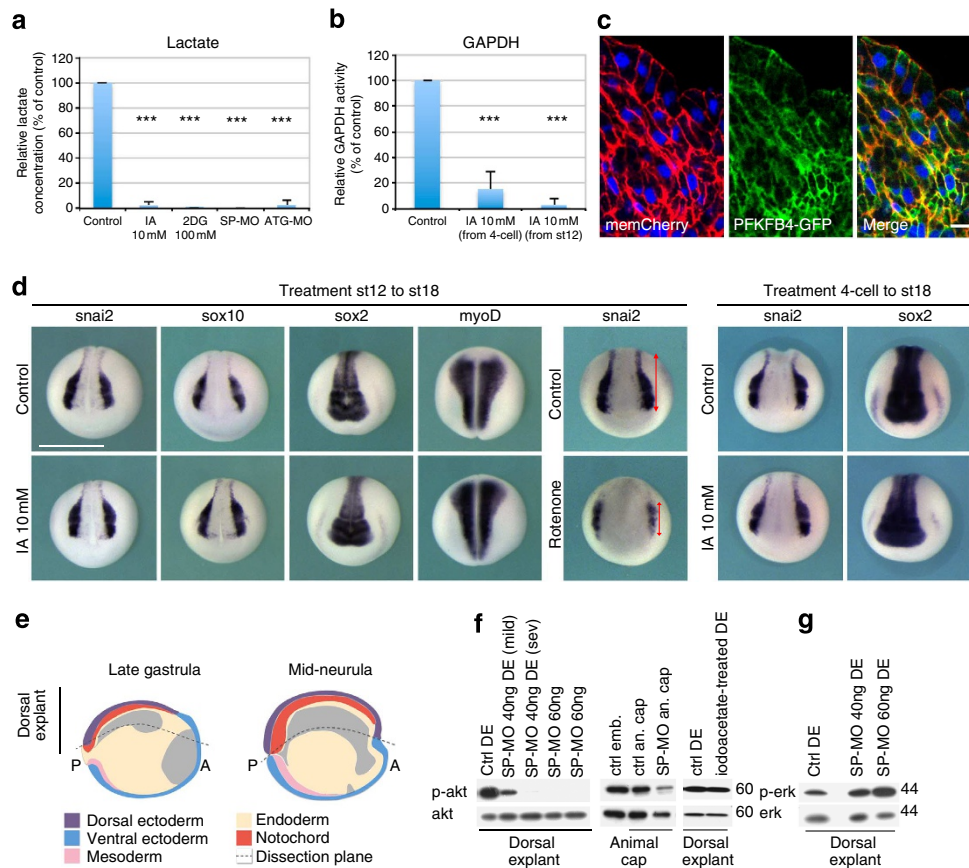


**Figure 2 | PFKFB4 controls Akt signalling *in vivo*, independently of glycolysis regulation.** (a,b) Lactate concentration (a) and GAPDH activity (b) confirmed glycolysis blockade with 2DG (100 mM) or IA (10 mM) (% of control sample value, 9 independent experiments with 10 embryos for each condition in each experiment; Student's *t*-test:  $P < 0.001$ . Error bars represent s.d.). Similar dosage in PFKFB4 morphants also shows efficient glycolysis blockade. (c) Subcellular localization of PFKFB4-GFP in dorsal ectoderm cells was restricted to the cytoplasm (membrane tagged-cherry-*fp*, *pfkfb4-gfp* injections, with nuclear DAPI staining, transverse section through neural plate, neural crest and ectoderm). Scale bar, 15  $\mu$ m. (d) Normal neurula patterning occurred when glycolysis was blocked by IA *in vivo*, either from four-cell stage to stage 18, or during neurulation (st12-st18) (similar results were obtained with 2DG, as shown in Supplementary Fig. 4). In contrast, a short treatment with the mitochondrial blocker rotenone (0.05  $\mu$ M) rapidly stopped neurulation and patterning. Scale bar, 1 mm. (e) Dorsal explants (DE) were dissected from either late gastrula (stage 12) or mid-neurula (stage 14) embryos (schematic sagittal view with dissection plane as dotted line, A; anterior, P; posterior). (f) Akt phosphorylation was decreased in DE or in animal caps (AC) following *pfkfb4* SP-MO injection at increasing doses (40 ng—embryos were sorted according to their mild or severe phenotype— or 60 ng). Akt phosphorylation was unchanged after glycolysis blockade. (g) Erk phosphorylation was present in DE following *pfkfb4* SP-MO injection. (f,g) At least three independent experiments were performed for each condition, all embryos from the same condition presented similar phenotypes as pictured.

expression of *pfkfb4* (6-phosphofructo-2-kinase/fructose-2,6-bisphosphatase isoform-4), gene coding a key regulator of glycolysis<sup>7,8</sup> (Supplementary Fig. 1), was increased in dorsal ectoderm during gastrulation and neurulation in frog and chick embryos (Fig. 1a,b; Supplementary Fig. 2). *Pfkfb4* late gastrula expression overlapped with the pattern of the neurectoderm marker *sox2*; while *pfkfb4* mid-neurula expression was restricted to the anterior neural folds, similar to neural border (*zic1*, *pax3*) and NC (*snail2*) markers, with a faint NP expression (Fig. 1a,b; Supplementary Fig. 2)<sup>13</sup>. *Pfkfb4* is the major isoform in dorsal tissues<sup>9</sup>. To address the role of PFKFB4, we validated *pfkfb4* translation and splice-blocking morpholinos (ATG/SP-MO, Fig. 1c,d; Supplementary Fig. 3). Morphant embryo morphology was normal until mid-neurula (stage 14), then the injected cells underwent a marked cell apoptosis and embryos died at late neurula stage (stage 18–20, Fig. 1e). This striking phenotype was strictly dependent on PFKFB4 depletion as a 'rescue' experiment, using coinjection of *pfkfb4* SP-MO with *pfkfb4*-encoding mRNA (messenger RNA) (insensitive to the morpholino), abolished cell death and restored normal development (Fig. 1e; 90% of morphants show increased cell death at stage 14, whereas only

45% of embryos do in the rescue situation). We concluded that PFKFB4 activity was essential for dorsal ectoderm survival during neurulation.

**Glycolysis blockade does not phenocopy PFKFB4 depletion.** In frog embryos, energy metabolism is mainly driven by amino acids fuelling the Krebs cycle until gastrulation<sup>10,11</sup>. However, vertebrate PFKFB enzymes are bifunctional kinases/phosphatases controlling fructose-6-phosphate reversible transformation into fructose-2,6-bisphosphate, a potent allosteric activator of the glycolysis rate-limiting enzyme phosphofructokinase-1 (PFK1, Supplementary Fig. 1)<sup>14–17</sup>. By controlling fructose-2,6-bisphosphate levels, PFKFBs regulate PFK1 activity, thereby controlling glycolysis rate<sup>7,8</sup>. Our observation of a key function for PFKFB4 in embryonic cell survival raised two non-exclusive hypotheses: either glycolysis played a specific function in dorsal ectoderm during neurulation or PFKFB4 played a non-metabolic role during dorsal development. To test the first hypothesis, we blocked glycolysis by two distinct pharmacological agents: 2-deoxyglucose (2DG, blocks glycolysis upstream of PFK1) or

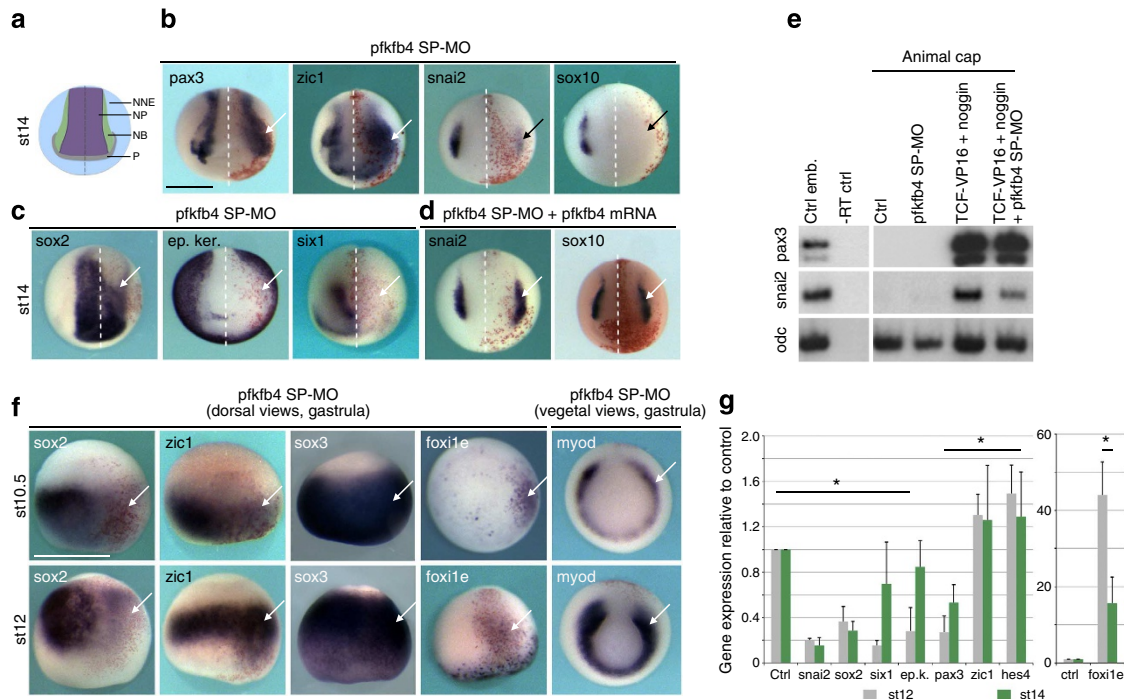


**Figure 3 | Pfkfb4 depletion blocks the early specification of dorsal ectoderm derivatives.** (a) Dorsal ectoderm-derived territories at mid-neurulation (stage 14, NNE, NB, NP, P as in Fig. 1a). (b,c) PFKFB4 morphant phenotype at mid-neurulation on NB (NC progenitors, *pax3* and *zic1*), early NC (*snail2* and *sox10*) and on NP (*sox2*), NNE (*ep. ker.*) and P (*six1*). A total of 998 embryos were analysed; the main phenotype is shown and a detailed statistical analysis is given in Supplementary Table 2. Dotted line indicates the mid-line, non-injected side on the left, injected side on the right (arrow, red dots indicate beta-galactosidase lineage tracing). Scale bar, 1 mm. (d) *Pfkfb4* SP-MO patterning phenotype was efficiently rescued by adding morpholino-insensitive *pfkfb4* mRNA. (e) Animal caps were induced to form NB and NC using Wnt activation (with TCF3-VP16) and bone morphogenetic protein blockade (with noggin). Similarly, PFKFB4 knockdown blocked NC induction (*snail2*), but not NB induction (*pax3*). (f) Ectoderm patterning defects arise as gastrulation is initiated (stage 10.5) in PFKFB4 morphants: *sox2* fails to be induced while *myod* remains roughly normal, in contrast, maternal genes and progenitor markers are maintained, expanded or activated ectopically (*sox3*, *zic1*, and *foxi1e*). (g) RT-qPCR quantification of specification markers (*snail2*, *sox2*, *six1*, and *ep.ker.*) and progenitor markers (*pax3*, *zic1*, *hes4* and *foxi1e*) in PFKFB4 morphant embryos, relative to control, during neurulation. *Foxi1e* showed very high differential levels in morphant DE compared with controls, as *foxi1e* expression, normally excluded from the dorsal side<sup>50</sup>, is retained in morphants. Analysis in whole embryos results in increased levels similar to whole-embryo pharmacological treatments (Fig. 4). At least three independent experiments were performed. A *t*-test was used to generate the *P* value ( $P \leq 0.01$ ) and error bars represent s.e.m.

iodoacetate (IA, inhibits GAPDH activity downstream of PFK1 (ref. 18)) (Supplementary Fig. 1). Glycolysis was efficiently blocked *in vivo*, by 2DG, IA or *pfkfb4* morpholinos (Fig. 2a,b; Supplementary Table 2). However, when embryos were treated with 2DG or IA, either from four-cell stage to late neurula stage (that is, reproducing the timing of morpholino injections) or only during neurulation, the embryos developed normally: their external morphology, the expression of NP, NC and paraxial mesoderm markers were normal (Fig. 2d; Supplementary Figs 4 and 8). No cell death was observed. In contrast, when the mitochondrial blocker rotenone was applied, rapid development arrest was observed: neural tube closure failed and gene expression was blocked (for example, *snail2* in NC, Fig. 2d). The embryos died rapidly. This indicated that embryo energy metabolism is mainly oxidative until neurulation, as reported for earlier cleavage stages<sup>10</sup>. Therefore, as dorsal ectoderm development proceeded normally when glycolysis was blocked, we concluded that the cell death observed after PFKFB4 depletion was not caused by insufficient glycolysis rate.

**PFKFB4 controls Akt phosphorylation *in vivo*.** To address the mechanism of PFKFB4-induced cell survival, we hypothesized that PFKFB4 depletion impaired Akt signalling, a critical player in cell survival<sup>19,20</sup>. We compared the levels of Akt S473-phosphorylation in control or morphant dorsal explants (DE) (Fig. 2e,f). Morphant DE displayed a strong, dose-dependent,

reduction of Akt phosphorylation. Similarly, blastula roof ectoderm (animal cap ectoderm) injected with *pfkfb4* morpholino displayed reduced Akt phosphorylation. In contrast, Akt phosphorylation was normal in IA-treated DE, indicating that glycolysis inhibition does not affect Akt signalling. To identify other potential perturbations in cell signalling and homeostasis after PFKFB4 depletion, we performed a global kinome analysis, using peptide arrays for 288 serine/threonine and tyrosine kinases<sup>21</sup>: no significant perturbation of main kinase activities was detected. Accordingly, we did not detect major changes in MAPK activation on PFKFB4 depletion in DE (Fig. 2g). Finally, as other glycolysis enzymes play roles in the nucleus<sup>22,23</sup>, we analysed PFKFB4 subcellular localization. PFKFB4-GFP fusions were injected in mild gain-of-function conditions *in vivo*. PFKFB4-GFP fluorescence intensity was quantified on NP sections, and compared with control GFP intensity. PFKFB4-GFP was located in the cytoplasm, no nuclear enrichment was seen (Fig. 2c, Supplementary Fig. 5). Altogether, we concluded that a major molecular consequence of PFKFB4 depletion was the defective activation of the Akt pathway, leading to morphant cell death. These data uncover the first glycolysis-independent role for PFKFB enzymes.

**PFKFB4 controls early neurula dorsal ectoderm specification.** We then addressed the role of this novel PFKFB4/Akt pathway in

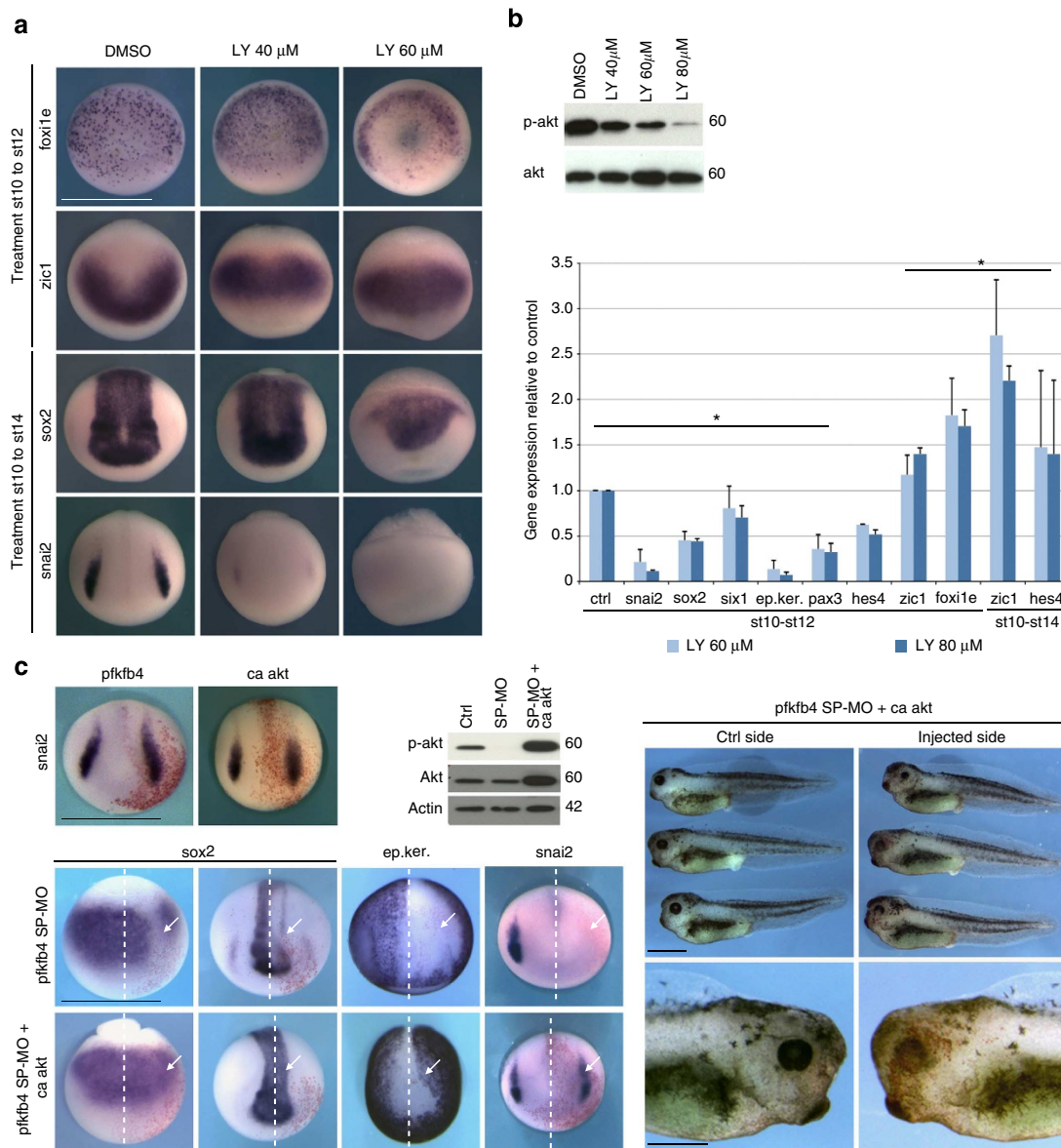


**Figure 4 | Akt signalling mediates PFKFB4 function in ectoderm early patterning *in vivo*.** (a,b) WISH and RT-qPCR analysis showed that pharmacological blockade of PI3K/Akt signalling *in vivo*, using increasing doses of LY294002, blocked ectoderm specification, while it maintained or increased progenitor marker expression. Three independent experiments were performed and error bars represent s.e.m. (*t*-test,  $P \leq 0.05$ ). Scale bar, 1 mm. (b) Decreased Akt phosphorylation confirmed LY294002 treatment efficiency. (c) PFKFB4 or constitutively active (ca) akt gain-of-function *in vivo* produced very modest expansions of ectoderm territories (here *snai2*). PFKFB4 morphant defects were efficiently rescued by ca akt coinjection, allowing normal embryo development, including neurulation and organogenesis. Akt phosphorylation was also restored. Swimming tadpoles developed normally and exhibit beta-galactosidase-labelled progeny of the injected blastomere. Scale bars, 1 mm. Six independent experiments were performed. For WISH, a total of 312 embryos were analysed; the main phenotype is shown and a detailed statistical analysis is given in Supplementary Table 2.

developing embryos. We first investigated why PFKFB4 depletion caused such marked embryonic death, by analysing morphant development before cell death. In early neurulas, critical patterning events define the prospective neural tube, NC and placodes from the NNE. Blocking patterning cues *in vivo*, for example, bone morphogenetic proteins, FGF or Wnt signals, does not result in cell death, but rather in increasing one cell fate at the expense of another<sup>24,25</sup>. However, we hypothesized that a global patterning defect, which would not allow alternative fate choice, would eventually result in cell apoptosis. We thus analysed the identity of the PFKFB4 morphant cells, before cell death (Fig. 3). At mid-neurulation (stage 14), unilateral morpholino injections showed increased expression of neural border progenitor markers

(compare injected and control sides): *zic1* showed robust expansion, *pax3* was more modest (Supplementary Table 2). In contrast, markers for specified NP (*sox2*), NC (*snai2* and *sox10*), placodes (*six1*) and NNE (*epidermal keratin*, *ep.ker.*), were absent in morphant areas (Fig. 3a–c, Supplementary Figs 3 and 8). This phenotype was efficiently rescued *in vivo* by restoring PFKFB4 activity in morphants (Fig. 3d, Supplementary Table 2). We confirmed these results using an *ex vivo* model of neural border and NC induction<sup>26</sup>. Both *pax3* and *snai2* were efficiently induced by activating Wnt signalling and inhibiting bone morphogenetic protein signalling in blastula ectoderm/animal cap assay<sup>27</sup>. In contrast, in the presence of *pfkfb4* morpholino, while *pax3* was activated, *snai2* induction was defective (Fig. 3e).

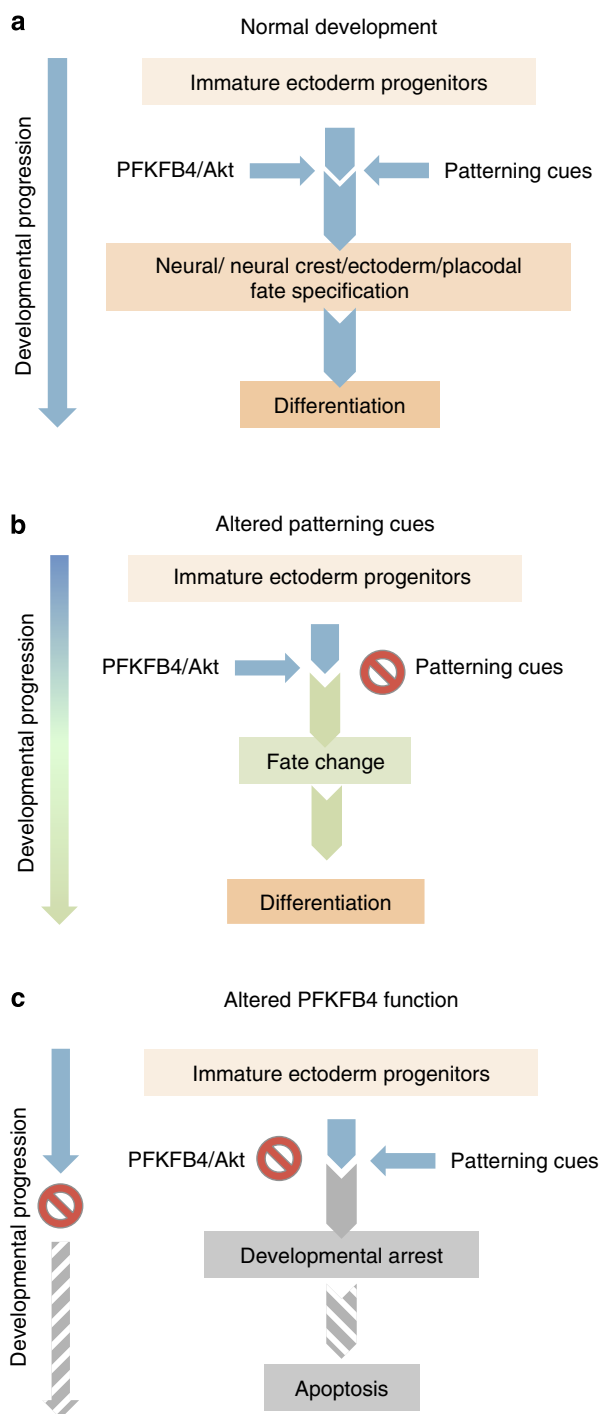


**Figure 5 | Model of PFKFB4 function during embryonic patterning.**

We propose that, during normal development, (a) PFKFB4/Akt-linked checkpoint allows developmental progression and patterning to occur. (b) If patterning signals are altered, it is known that developing progenitors follow alternative fates. (c) In contrast, if PFKFB4/Akt pathway is defective, no viable developmental alternative is offered to progenitor cells, which arrest their developmental programme at progenitor stage and eventually undergo apoptosis.

Altogether, these results indicated a global failure to specify both neural and non-neural dorsal ectoderm fates during early neurulation, before apoptosis. In contrast, the expression of markers for neural border progenitors<sup>28</sup> was either unaffected or enlarged. This suggested that earlier modulation of gene

expression in immature ectoderm cells may account for the phenotype observed during neurulation. We further analysed the initiation of dorsal progenitors specification during gastrulation, that is, 18 h earlier. While *sox2* failed to be induced in the NP, *zic1*, a direct target of organizer signals<sup>29</sup>, was normal or expanded (Fig. 3f, Supplementary Table 2). In addition, the maternal gene *sox3* was normal until mid-neurula stage (Fig. 3f) and the NNE progenitor marker *foxi1e* was precociously activated (early gastrulation), then ectopically expressed (late gastrulation, Fig. 3f). Paraxial mesoderm progenitor development (*myod*) was roughly normal (Fig. 3f). Finally, quantitative PCR with reverse transcription (RT-qPCR) analysis of morphant DE also showed increased progenitor marker expression (*zic1*, *hes4* and *foxi1e*) and decreased specification marker expression (*snail2*, *sox2* and *six1*), when compared with control (Fig. 3g). The global level for the non-neural ectoderm marker *ep.ker.* was not as significantly decreased at stage 14 (Supplementary Table 2). Collectively, these data demonstrate that PFKFB4 activity is essential for the progression from a progenitor cell status towards specified ectoderm fates *in vivo*. In addition, when this activity is impaired, it is followed by arrest in the developmental cascade of gene expression (developmental arrest, around stages 10.5–12), then, several hours later, by apoptosis (around stage 14–15).

**Akt acts downstream of PFKFB4 in dorsal development.** As PFKFB4 depletion affected Akt phosphorylation, we tested the consequences of Akt signalling inhibition on ectoderm specification *in vivo*, using the PI3-kinase pharmacological inhibitor LY294002 (ref. 30). As early treatments blocked gastrulation as previously reported<sup>30</sup>, we treated embryos with increasing doses shortly after dorsal blastopore lip formation until early or mid-neurula stage (Fig. 4a,b). Akt phosphorylation blockade was monitored by western blotting. As in PFKFB4 morphants, both using whole-mount *in situ* hybridization (WISH) and RT-qPCR, we observed severe loss of *snail2*, defective *sox2*, *six1* and *ep.ker.* expression, and elevated levels of *zic1*, *hes4* and *foxi1e* (Fig. 4a,b; Supplementary Fig. 8). Although minor differences were observed in the intensity and timing of gene modulations (see *hes4* late increase), the phenotype of PFKFB4 morphants and LY294002-treated neurulas was thus similar. We further compared the effects of PFKFB4 and Akt gain-of-function *in vivo*: in both cases, very mild NP and NC expansions were observed while NNE was normal (Fig. 4c), indicating that neither PFKFB4 nor Akt increased levels modified significantly fate choices in dorsal ectoderm.

Importantly, we then tested the epistasis relationships between PFKFB4 and Akt, as those two enzyme activities have not been associated previously. Constitutively active (*ca*) *akt* restored Akt phosphorylation levels in PFKFB4 morphants (Fig. 4c). Unilateral coinjection of *pfkfb4* morpholino with *ca akt* mRNA resulted in a spectacular rescue of neural and non-neural markers expression (Fig. 4c; Supplementary Fig. 8), allowing neural tube closure and further development until tadpole stage (Fig. 4c). Both neurulas and swimming tadpoles exhibited healthy lineage-traced cells deriving from the blastomere coinjected with *pfkfb4* SP-MO and *ca akt*. This last result indicated that the mechanism of PFKFB4 critical activity on ectoderm patterning and survival, is mainly dependent on modulating Akt signalling.

**Apoptosis can be uncoupled from early patterning defects.**

Finally, we confirmed that this novel PFKFB4/Akt function primarily controls ectoderm early patterning and that, if blocked, it secondarily results in cell death. We prevented apoptosis initiation using the antiapoptotic factor Bcl-XL, which acts early in the apoptotic cascade<sup>31</sup>. *Bcl-xl* mRNA expression in PFKFB4

morphants prevented mid-neurula stage cell death very efficiently, but did not restore neural, neural crest and ectoderm patterning defects (Supplementary Fig. 6). Although we cannot completely rule out the existence of a preapoptotic state in the PFKFB4 morphant cells, this result strongly suggests that the observed early patterning deficiencies are not the consequence of an apoptotic programme initiation, but rather the cause of cell death. Altogether, our results show that PFKFB4/Akt is critical for ectoderm patterning as gastrulation is initiated and that this function cannot be bypassed by adoption of an alternative fate, eventually resulting in cell apoptosis.

## Discussion

Our study uncovered a novel function for PFKFB4 in cell fate programming, independent from its classical role in glycolysis regulation. Frog embryo oxidative metabolism allowed experimental uncoupling of glycolysis from other PFKFB4 activities. We showed that PFKFB4 was essential for a novel checkpoint in progenitor cell developmental progression, via Akt signalling (Model, Fig. 5a). We propose that altering this checkpoint interferes with the cascade of developmental events, causing a developmental arrest: cells remain in a progenitor state. During embryogenesis, when patterning cues are altered, embryonic progenitor cells are diverted towards alternative cell fates, without such arrest: this results in the development of modified but healthy tissues (Fig. 5b). Here, the PFKFB4/Akt-linked checkpoint does not alter cell fate equilibrium, but rather acts on all dorsal ectoderm fates simultaneously and allows the developmental progression of progenitor cells: our findings show that Akt is essential for maintaining normal development (Fig. 5c). We propose that the arrest in development of progenitors, that cannot be resolved, then activates apoptotic elimination of the defective cells. The molecular link between PFKFB4 and Akt signalling remains elusive. Coimmunoprecipitation experiments failed to pull down a protein complex (Supplementary Fig. 7), suggesting indirect relationships. Further studies will explore the nature of these interactions that may involve non-conventional activities for PFKFB4 or interactions between PFKFB4 and upstream regulators of Akt.

Whereas numerous studies highlight the importance of metabolic regulations in various normal and pathological cell processes<sup>1–6,32–36</sup>, few studies have explored novel roles of classical metabolism regulators<sup>4,37</sup>. Our results demonstrate that normal, cytoplasmic, PFKFB4 levels are a prerequisite for ectoderm development and survival. The enrichment of *pfkfb4* expression in frog and chick dorsal ectoderm during gastrulation and neurulation suggested that these cells might display an acute sensitivity to PFKFB4/Akt levels during their early specification, although other cell types that express lower levels of *pfkfb4* or other *pfkfb* isoforms, may also respond to similar regulations. In addition, it will be interesting to compare this novel PFKFB4/Akt signalling to PI3K/Akt/GSK3 signalling affecting early dorsal axis formation during cleavage stages<sup>38</sup>. Future work will address PFKFB4/Akt signalling mechanisms, in dorsal ectoderm and other contexts of stem cell differentiation.

## Methods

All reagents are listed in Supplementary Table 1. Sample size is chosen to be statistically significant, at least three independent experiments are conducted for each condition, series of injected embryos are at least of 20 embryos. All phenotypes shown are the most frequent phenotype for each experiment. All details on the statistical analysis and total sample counts are given in Supplementary Table 2.

**Embryo injections.** *Xenopus laevis* and *Gallus gallus* embryos were obtained, staged and dissected using standard procedures<sup>39,40</sup>. The care and use of animals used here was strictly applying European and National Regulation for the

Protection of Vertebrate Animals used for Experimental and other Scientific Purposes in force (facility licence #C91-471-108 given by the Direction Départementale de Protection de la Population, Courcouronnes, France).

*X. laevis* embryos were obtained by *in vitro* fertilization using standard procedures and were staged according to Niewkoop and Faber developmental table<sup>39,41</sup>. For *in vivo* analysis, embryos were injected unilaterally at four-cell stage and grown until stages 10–40. Nuclear-targeted beta-galactosidase mRNA was coinjected as a lineage tracer with each mRNA or MOs. Beta-galactosidase activity was revealed in red, indicating the injected side, before WISH. For whole-embryo injections, the two blastomeres were injected at two-cell stage in the animal pole. Animal cap explants were cut at blastula stage 9 and dorsal explants at either late gastrula stage 12 or mid-neurula stage 14. mRNAs used for microinjection were obtained by *in vitro* transcription of plasmids containing the desired cDNA using the mMessage mMachine SP6 or T7 kits (Ambion) and purified on G50 sephadex spin columns. The following plasmids were used: *bcl-xl*<sup>42</sup>, *ca akt*<sup>43</sup>, *memcherry*<sup>44</sup>, *nlacZ*<sup>45</sup>, *noggin*<sup>46</sup>, *pfkfb4* (this study), *pfkfb4-gfp* (this study) and *tcf3VP16-GR*<sup>47</sup>. PFKFB4 silencing was performed using translation-blocking or splice-blocking antisense morpholino oligonucleotides (GeneTools, this study). The efficiency and specificity of the MOs was tested by <sup>35</sup>S-labelled *in vitro* transcription-and-translation reaction using TNT kit (Promega) or RT-qPCR. Reagents, plasmids and morpholinos are further described in Supplementary Table 1.

**Whole-mount *in situ* hybridization (WISH).** Embryos were fixed and prepared for WISH according to a fast protocol optimized for superficial structures<sup>48</sup>. Antisense digoxigenin-labelled RNA probes were used at a final concentration of 1 µg ml<sup>-1</sup>. The following probes were used: *ep. ker.*<sup>49</sup>, *foxi1e*<sup>50</sup>, *hes4* (ref. 51), *myod*<sup>52</sup>, *pax3* (ref. 26), *X. laevis pfkfb4* (this study), *chick pfkfb4* (this study), *six1* (ref. 53), *snai2* (ref. 54), *sox10* (ref. 55) and *zic1* (ref. 56). All NCBI Reference Sequences are listed in Supplementary Table 1. Additional pictures showing groups of embryos are presented in Supplementary Fig. 8.

**Coimmunoprecipitation and western blotting.** Immunoprecipitation and western blot analysis were performed as previously described<sup>57</sup>. In brief, lysates of HEK293T or 5–10 embryos were prepared with cold lysis buffer. Immunoprecipitations were conducted on HEK293T cell lysates at 4 °C for 3 h with anti-HA antibody and protein-A sepharose beads (Sigma). Immunoprecipitates were washed with lysis buffer three times and analysed by western blot. All antibodies were diluted in 5% skimmed milk. The concentration and source of all antibodies used for western blotting are detailed in Supplementary Table 1. Full scans of blots accompanied by the position of molecular weight markers are shown in Supplementary Fig. 9.

**Semi-quantitative and RT-qPCR.** Embryos were lysed in proteinase K-containing lysis buffer, followed by DNase treatment and reverse transcription<sup>39</sup>. RT-qPCR was performed according to standard procedures using MIQE recommendations. *Eflα* and *odc* were used as controls. Results are shown relative to expression in sibling control samples. The sequences of all primers used in this study are listed in Supplementary Table 1.

**Glycolysis measurement.** GAPDH activity and lactate concentration were measured on lysates from 20 sibling embryos using KD-Alert GAPDH kit (Life Technologies) and L-Lactate Kit (Abcam).

**Cell death.** Embryos were fixed in 3.7% formaldehyde in PBS and dehydrated in methanol. Apoptotic cells were visualized using acridine orange staining or cleaved caspase-3 immunostaining<sup>42</sup>. The concentration and source of reagents and antibodies are detailed in Supplementary Table 1.

**Imaging.** Confocal images were obtained from cryosections of embryos expressing PFKFB4-GFP, GFP or memCherryFP (Leica SP5, 60X/1.4)<sup>58</sup>. Subcellular GFP fluorescence (in pixel intensities) was measured on a total of 60 cells per condition (ImageJ software).

## References

- Hirschhaeuser, F., Sattler, U. G. A. & Mueller-Klieser, W. Lactate: a metabolic key player in cancer. *Cancer Res.* **71**, 6921–6925 (2011).
- Schoors, S. *et al.* Partial and transient reduction of glycolysis by PFKFB3 blockade reduces pathological angiogenesis. *Cell Metab.* **19**, 37–48 (2014).
- De Bock, K. *et al.* Role of PFKFB3-driven glycolysis in vessel sprouting. *Cell* **154**, 651–663 (2013).
- Yang, W. *et al.* PKM2 phosphorylates histone H3 and promotes gene transcription and tumorigenesis. *Cell* **150**, 685–696 (2012).
- Hitosugi, T. *et al.* Phosphoglycerate mutase 1 coordinates glycolysis and biosynthesis to promote tumor growth. *Cancer Cell* **22**, 585–600 (2012).



6. Favaro, E. *et al.* Glucose utilization via glycogen phosphorylase sustains proliferation and prevents premature senescence in cancer cells. *Cell Metab.* **16**, 751–764 (2012).
7. Okar, D. A. *et al.* PFK-2/FBPase-2: maker and breaker of the essential biofactor fructose-2,6-bisphosphate. *Trends Biochem. Sci.* **26**, 30–35 (2001).
8. Rider, M. H. *et al.* 6-Phosphofructo-2-kinase/fructose-2,6-bisphosphatase: head-to-head with a bifunctional enzyme that controls glycolysis. *Biochem. J.* **381**, 561 (2004).
9. Pegoraro, C., Maczkowiak, F. & Monsoro-Burq, A. H. Pfkfb (6-phosphofructo-2-kinase/fructose-2,6-bisphosphatase) isoforms display a tissue-specific and dynamic expression during *Xenopus laevis* development. *Gene Expr. Patterns* **13**, 203–211 (2013).
10. Vastag, L. *et al.* Remodeling of the metabolome during early frog development. *PLoS ONE* **6**, e16881 (2011).
11. Jorgensen, P., Steen, J. A. J., Steen, H. & Kirschner, M. W. The mechanism and pattern of yolk consumption provide insight into embryonic nutrition in *Xenopus*. *Development* **136**, 1539–1548 (2009).
12. Plouhinec, J.-L. *et al.* Pax3 and Zic1 trigger the early neural crest gene regulatory network by the direct activation of multiple key neural crest specifiers. *Dev. Biol.* **386**, 461–472 (2014).
13. Rex, M. *et al.* Dynamic expression of chicken Sox2 and Sox3 genes in ectoderm induced to form neural tissue. *Dev. Dyn.* **209**, 323–332 (1997).
14. Pilkis, S. J., El-Maghrabi, M. R., Pilkis, J., Claus, T. H. & Cumming, D. A. Fructose 2,6-bisphosphate. A new activator of phosphofructokinase. *J. Biol. Chem.* **256**, 3171–3174 (1981).
15. Uyeda, K., Furuya, E. & Luby, L. J. The effect of natural and synthetic D-fructose 2,6-bisphosphate on the regulatory kinetic properties of liver and muscle phosphofructokinases. *J. Biol. Chem.* **256**, 8394–8399 (1981).
16. Choi, I.-Y., Wu, C., Okar, D. A., Lange, A. J. & Gruetter, R. Elucidation of the role of fructose 2,6-bisphosphate in the regulation of glucose fluxes in mice using in vivo <sup>13</sup>C NMR measurements of hepatic carbohydrate metabolism. *Eur. J. Biochem.* **269**, 4418–4426 (2002).
17. Wu, C. *et al.* Enhancing hepatic glycolysis reduces obesity: differential effects on lipogenesis depend on site of glycolytic modulation. *Cell Metab.* **2**, 131–140 (2005).
18. Wu, M. *et al.* Multiparameter metabolic analysis reveals a close link between attenuated mitochondrial bioenergetic function and enhanced glycolysis dependency in human tumor cells. *Am. J. Physiol. Cell Physiol.* **292**, C125–C136 (2007).
19. Manning, B. D. & Cantley, L. C. AKT/PKB signaling: navigating downstream. *Cell* **129**, 1261–1274 (2007).
20. Datta, S. R., Brunet, A. & Greenberg, M. E. Cellular survival: a play in three Akts. *Genes Dev.* **13**, 2905–2927 (1999).
21. Lemeer, S. *et al.* Protein-tyrosine kinase activity profiling in knock down zebrafish embryos. *PLoS ONE* **2**, e581 (2007).
22. Yalcin, A. *et al.* Nuclear targeting of 6-phosphofructo-2-kinase (PFKFB3) increases proliferation via cyclin-dependent kinases. *J. Biol. Chem.* **284**, 24223–24232 (2009).
23. Yang, W. *et al.* Nuclear PKM2 regulates  $\beta$ -catenin transactivation upon EGFR activation. *Nature* **480**, 118–122 (2011).
24. Patthey, C. & Gunhaga, L. Signaling pathways regulating ectodermal cell fate choices. *Exp. Cell Res.* **321**, 11–16 (2014).
25. Pegoraro, C. & Monsoro-Burq, A. H. Signaling and transcriptional regulation in neural crest specification and migration: lessons from *Xenopus* embryos. *WIREs Dev. Biol.* **2**, 247–259 (2013).
26. Monsoro-Burq, A.-H., Wang, E. & Harland, R. Msx1 and Pax3 cooperate to mediate FGF8 and WNT signals during *Xenopus* neural crest induction. *Dev. Cell.* **8**, 167–178 (2005).
27. de Croz e, N., Maczkowiak, F. & Monsoro-Burq, A. H. Reiterative AP2a activity controls sequential steps in the neural crest gene regulatory network. *Proc. Natl Acad. Sci. USA* **108**, 155–160 (2011).
28. Milet, C., Maczkowiak, F., Roche, D. D. & Monsoro-Burq, A. H. Pax3 and Zic1 drive induction and differentiation of multipotent, migratory, and functional neural crest in *Xenopus* embryos. *Proc. Natl Acad. Sci. USA* **110**, 5528–5533 (2013).
29. Aruga, J. The role of Zic genes in neural development. *Mol. Cell. Neurosci.* **26**, 205–221 (2004).
30. Carballada, R., Yasuo, H. & Lemaire, P. Phosphatidylinositol-3 kinase acts in parallel to the ERK MAP kinase in the FGF pathway during *Xenopus* mesoderm induction. *Development* **128**, 35–44 (2001).
31. Youle, R. J. & Strasser, A. The BCL-2 protein family: opposing activities that mediate cell death. *Nat. Rev. Mol. Cell Biol.* **9**, 47–59 (2008).
32. Ochocki, J. D. & Simon, M. C. Nutrient-sensing pathways and metabolic regulation in stem cells. *J. Cell Biol.* **203**, 23–33 (2013).
33. Heiden, M. G. V., Cantley, L. C. & Thompson, C. B. Understanding the Warburg Effect: The Metabolic Requirements of Cell Proliferation. *Science* **324**, 1029–1033 (2009).
34. Almeida, A., Bolaños, J. P. & Moncada, S. E3 ubiquitin ligase APC/C-Cdh1 accounts for the Warburg effect by linking glycolysis to cell proliferation. *Proc. Natl Acad. Sci. USA* **107**, 738–741 (2010).
35. Esen, E. *et al.* WNT-LRP5 Signaling Induces Warburg Effect through mTORC2 Activation during Osteoblast Differentiation. *Cell Metab.* **17**, 745–755 (2013).
36. Chan, O., Burke, J. D., Gao, D. F. & Fish, E. N. The chemokine CCL5 regulates glucose uptake and AMP kinase signaling in activated T cells to facilitate chemotaxis. *J. Biol. Chem.* **287**, 29406–29416 (2012).
37. Nicholls, C., Li, H. & Liu, J.-P. GAPDH: a common enzyme with uncommon functions. *Clin. Exp. Pharmacol. Physiol.* **39**, 674–679 (2012).
38. Peng, Y. *et al.* Phosphatidylinositol 3-kinase signaling is involved in neurogenesis during *Xenopus* embryonic development. *J. Biol. Chem.* **279**, 28509–28514 (2004).
39. Sive, H. L., Grainger, R. M. & Harland, R. M. *Early Development of Xenopus laevis: A Laboratory Manual* (Cold Spring Harbor Laboratory Press, 2000).
40. Monsoro-Burq, A. & Le Douarin, N. Left-right asymmetry in BMP4 signalling pathway during chick gastrulation. *Mech. Dev.* **97**, 105–108 (2000).
41. Nieuwkoop, P. D. & Faber, J. *Normal Table of Xenopus laevis (Daudin): A Systematical and Chronological Survey of the Development from the Fertilized Egg Till the End of Metamorphosis* (Garland Pub., 1994).
42. Juraver-Geslin, H. A., Ausseil, J. J., Wassef, M. & Durand, B. C. Barhl2 limits growth of the diencephalic primordium through Caspase3 inhibition of beta-catenin activation. *Proc. Natl Acad. Sci. USA* **108**, 2288–2293 (2011).
43. Peyssonnaud, C., Provot, S., Felder-Schmittbuhl, M. P., Calothy, G. & Eyche, A. Induction of postmitotic neuroretina cell proliferation by distinct Ras downstream signaling pathways. *Mol. Cell Biol.* **20**, 7068–7079 (2000).
44. Griffin, B. A., Adams, S. R. & Tsien, R. Y. Specific covalent labeling of recombinant protein molecules inside live cells. *Science* **281**, 269–272 (1998).
45. Gammill, L. S. & Sive, H. Coincidence of otx2 and BMP4 signaling correlates with *Xenopus* cement gland formation. *Mech. Dev.* **92**, 217–226 (2000).
46. Lamb, T. M. & Harland, R. M. Fibroblast growth factor is a direct neural inducer, which combined with noggin generates anterior-posterior neural pattern. *Development* **121**, 3627–3636 (1995).
47. Yang, J., Tan, C., Darken, R. S., Wilson, P. A. & Klein, P. S. Beta-catenin/Tcf-regulated transcription prior to the midblastula transition. *Development* **129**, 5743–5752 (2002).
48. Monsoro-Burq, A. H. A rapid protocol for whole-mount in situ hybridization on *Xenopus* embryos. *CSH Protoc.* doi:10.1101/pdb.prot4809 (2007).
49. Bradley, R. S., Espeseth, A. & Kintner, C. NF-protocadherin, a novel member of the cadherin superfamily, is required for *Xenopus* ectodermal differentiation. *Curr. Biol.* **8**, 325–334 (1998).
50. Mir, A. *et al.* FoxI1e activates ectoderm formation and controls cell position in the *Xenopus* blastula. *Development* **134**, 779–788 (2007).
51. Davis, R. L., Turner, D. L., Evans, L. M. & Kirschner, M. W. Molecular targets of vertebrate segmentation: two mechanisms control segmental expression of *Xenopus* hairy2 during somite formation. *Dev. Cell* **1**, 553–565 (2001).
52. Hopwood, N. D., Pluck, A. & Gurdon, J. B. MyoD expression in the forming somites is an early response to mesoderm induction in *Xenopus* embryos. *EMBO J.* **8**, 3409–3417 (1989).
53. Brugmann, S. A., Pandur, P. D., Kenyon, K. L., Pignoni, F. & Moody, S. A. Six1 promotes a placodal fate within the lateral neurogenic ectoderm by functioning as both a transcriptional activator and repressor. *Development* **131**, 5871–5881 (2004).
54. Grammer, T. C., Liu, K. J., Mariani, F. V. & Harland, R. M. Use of large-scale expression cloning screens in the *Xenopus laevis* tadpole to identify gene function. *Dev. Biol.* **228**, 197–210 (2000).
55. Aoki, Y. *et al.* Sox10 regulates the development of neural crest-derived melanocytes in *Xenopus*. *Dev. Biol.* **259**, 19–33 (2003).
56. Mizuseki, K., Kishi, M., Matsui, M., Nakanishi, S. & Sasai, Y. *Xenopus* Zic-related-1 and Sox-2, two factors induced by chordin, have distinct activities in the initiation of neural induction. *Development* **125**, 579–587 (1998).
57. Hmitou, I., Druillennec, S., Valluet, A., Peyssonnaud, C. & Eyche, A. Differential regulation of B-raf isoforms by phosphorylation and autoinhibitory mechanisms. *Mol. Cell Biol.* **27**, 31–43 (2007).
58. Fagotto, F. & Brown, C. M. in *Wnt Signaling*. (ed. Vincan, E.) 363–380 (Humana Press, 2009) at [http://link.springer.com.gate1.inist.fr/protocol/10.1007/978-1-60327-469-2\\_23](http://link.springer.com.gate1.inist.fr/protocol/10.1007/978-1-60327-469-2_23).

## Acknowledgements

We are grateful to D. Zala for advice on GAPDH measurement, to B. Durand for the gift of Bcl-XL plasmid and critical reading of the manuscript and to the Monsoro-Burq lab members for their continuous support. We also thank Institut Curie animal and imaging facilities. This work was funded by grants to A.H.M.-B. (ATIP PLUS CNRS, Agence Nationale pour la Recherche, Programme Blanc CRESTNET; Association pour la Recherche Contre le Cancer (ARC), Fondation pour la Recherche M dicale, PRES Universud, Attractivit  Universit  Paris Sud). C.P. was an Institut Curie and ARC PhD fellow; A.L.F. was a PhD fellow of the French Ministry for Research and Education (MENRT) and Fondation Pour la Recherche M dicale (FDT20140930900).

**Author contributions**

C.P., A.L.F., F.M., C. Po. and A.H.M.-B. have designed, conducted and analysed the experiments. C.P., A.L.F., F.M., C. Po., A.E. and A.H.M.-B. have discussed the results and written the manuscript.

**Additional information**

**Supplementary Information** accompanies this paper at <http://www.nature.com/naturecommunications>

**Competing financial interests:** The authors declare no competing financial interests.

**Reprints and permission** information is available online at <http://npg.nature.com/reprintsandpermissions/>

**How to cite this article:** Pegoraro, C. *et al.* PFKFB4 controls embryonic patterning via Akt signalling independently of glycolysis. *Nat. Commun.* 6:5953 doi: 10.1038/ncomms6953 (2015).